Supporting Information

A Novel Copper Metal-Organic Framework Catalyst for the Highly Efficient Conversion of CO₂ with Propargylic Amines

Xiao Xu, Zhentao Li, Huilin Huang, Xu Jing* and Chunying Duan

State Key Laboratory of Fine Chemicals, Zhang Dayu College of Chemistry, Dalian University of Technology, 116024, P. R. China.

E-mail: xjing@dlut.edu.cn

1. Experimental Section.

2. Single Crystal X-ray Crystallography.

3. Characterizations of Catalysts.

4. The Summary of MOFs Used in Cycloaddition of Propargylamines.

5. Catalysis Details.

6. References

1. Experimental Section.

Materials and methods

All substrates were used as received from commercial suppliers unless otherwise stated. Chemicals were purchased from Sigma-Aldrich, Chempur, TCI, or Alfa Aesar. Carbon dioxide (99.995%) was purchased from the Dalian Institute of Special Gases and used as received. The ligand **TSP** was synthesized according to the previously reported procedure.[1]

^{1}H NMR data were collected on a Varian DLG400 MHz spectrometer at ambient temperature. FT-IR spectra were recorded as KBr pellets on JASCO FT/IR-430 spectrometer. The powder XRD diffractograms were obtained on a Rigaku D/Max-2400 X-ray diffractometer with a sealed Cu tube (λ = 1.54178 Å). IR spectra were recorded as KBr pellets on a NEXUS instrument. Thermogravimetric analyses (TGA) were performed at a ramp rate of 10 °C/min in a nitrogen flow with an SDTQ600 instrument. Confocal Laser Scanning Microscopy micrographs were collected by Olympus Fluoview FV1000 with λ_{ex} = 617 nm. Liquid UV-*vis* spectra were performed on a TU-1900 spectrophotometer. The solid UV-*vis* spectra were recorded on a Hitachi U-4100 UV-*vis*-NIR spectrophotometer. The microstructure and morphology observations of samples were performed with a scanning electron microscope (SEM) of HITACHI UHR FE-SEM SU8220.

Preparation

(1) Synthesis of ligand **TSP**

A mixture of 1,3,5-Triacetylbenzene (0.2 g, 1 mmol), thiosemicarbazide (0.3 g, 3.3 mmol), and 5d acetic acid in 40 mL of methanol was stirred at 80 °C for 24 h. Then,

a white product was isolated by filtration and washed with ether three times to get dry products. Yield: 90%, 0.38 g.

(2) Synthesis of compound Cu-**TSP**

In a glass tube, **TSP** (4.2 mg) was dissolved in DMF (2.0 mL) and then 10 mL of a DMF/CH$_3$CN solution (1/8 v/v) was carefully layered followed by a layer of Cu(CH$_3$CN)$_4$BF$_4$ (4.7 mg) dissolved in CH$_3$CN (2.0 mL). The container was covered and stored in the dark for the slow diffusion of the reactants at room temperature, to afford pale yellow crystals within 3 weeks. The catalysts were soaked in ethanol and ether for guest molecular exchange. Yield: 40% (based on Cu).

2. Single Crystal X-ray Crystallography

Single-Crystal Analysis. X-ray intensity data were carried out on a Bruker SMART APEX charge-coupled device-based diffractometer (Mo Kα radiation, λ 0.71073 Å) with the SAINT and SMART programs. The SAINT software was used in the data integration and reduction. Empirical absorption correction, which was applied to the collected reflection, worked with SADABS. SHELXTL was used to solve the structures in direct methods, which was refined on F^2 by the full-matrix least-squares method with the program SHELXL-97.[2]

In the structural refinement of Cu-**TSP**, all of the non-hydrogen atoms were refined anisotropically. The hydrogen atoms within the ligand backbones were fixed geometrically at calculated distances and allowed to ride on the parent non-hydrogen atoms. The SQUEEZE subroutine in PLATON was used.[3]

Table S1. Crystal data and structure refinements.

| Compound	Cu-**TSP**
Empirical formula	$C_{20}H_{16}CuN_{12}S_4$
Formula weight	616.23
Temperature/K	120.0
Crystal system	cubic
Space group	I-43d
a/Å	29.0808(19)
b/Å	29.0808(19)
c/Å	29.0808(19)
$\alpha/°$	90
$\beta/°$	90
$\gamma/°$	90
Volume/Å^3	24593(5)
Z	12
$\rho_{calc}g/cm^3$	0.499
μ/mm^{-1}	0.380
F(000)	3756.0
Crystal size/mm^3	$0.08 \times 0.06 \times 0.05$
Radiation	MoKα (λ = 0.71073)
2 theta range for data collection/°	4.43 to 46.558
Index ranges	$-31 \leq h \leq 32, -32 \leq k \leq 31, -29 \leq l \leq 28$
Reflections collected	34109
Independent reflections	2965 [R_{int} = 0.0984, R_{sigma} = 0.0489]
Data/restraints/parameters	2965/0/85
Goodness-of-fit on F^2	1.136
Final R indexes [I>=2σ (I)]	R_1 = 0.0721, wR_2 = 0.2112
Final R indexes [all data]	R_1 = 0.0944, wR_2 = 0.2257
Largest diff. peak/hole / e Å^{-3}	0.34/-0.40
CCDC number	2160451
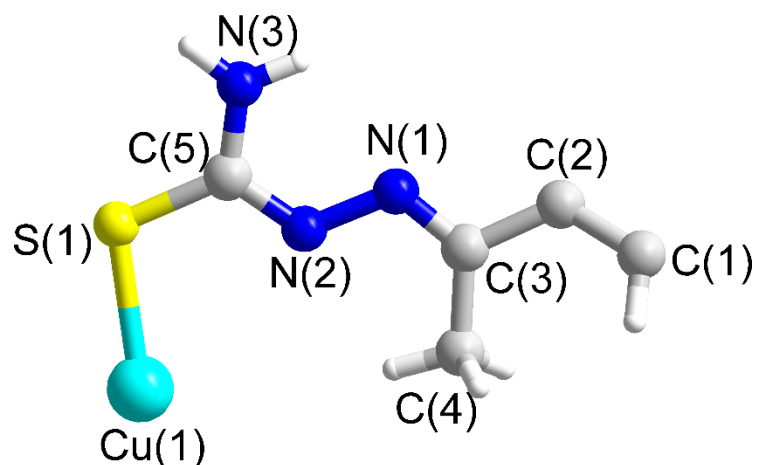
Figure S1. Asymmetric unit of Cu-**TSP**.

Selected bond distances (Å): Cu(1)-S(1) 2.325(2), S(1)-C(5) 1.709(10), N(2)-N(1) 1.390(11), N(2)-C(5) 1.298(12), N(1)-C(3) 1.244(12), N(3)-C(5) 1.321(12), C(3)-C(4) 1.464(16), C(3)-C(2) 1.476(14), C(2)-C(1) 1.393(15).
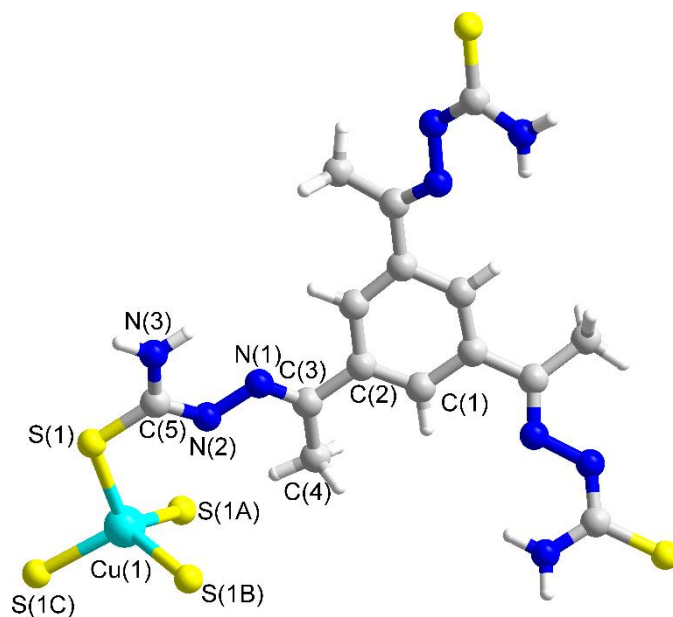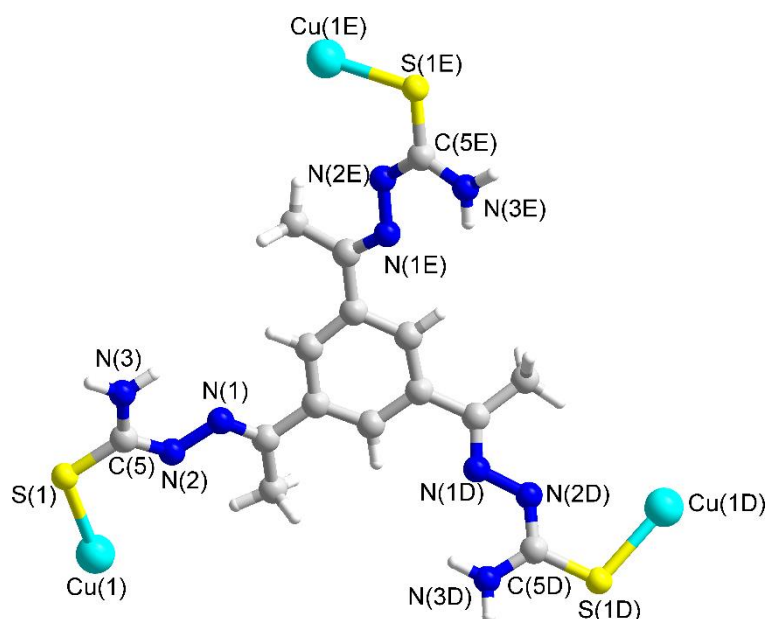

Figure S2 (a) Coordination geometry of the Cu (1) atom in Cu-**TSP**.

Cu-S bond distances (Å) and angles (°): Cu(1)-S(1) 2.325(2), Cu(1)-S(1A) 2.325(2), Cu(1)-S(1B) 2.325(2), Cu(1)-S(1C) 2.325(2); S(1A)-Cu(1)-S(1B) 105.06(6), S(1)-Cu(1)-S(1A) 105.06(6), S(1)-Cu(1)-S(1B) 118.71(12), S(1B)-Cu(1)-S(1C) 105.06(6),

S(1)-Cu(1)-S(1C) 105.06(6), S(1A)-Cu(1)-S(1C) 118.71(12). Symmetry Code: A: 1-x,

1.5-y, z; B: 1..25-y, 0.25+x, 0.75-z; C: -0.25+y, 1.25-x, 0.75-z.

Figure S3 Coordination geometry of **TSP** in Cu-**TSP**.

Selected bond distances (Å): Cu(1)-S(1) 2.325(2), S(1)-C(5) 1.709(10), N(2)-N(1)

1.390(11), N(2)-C(5) 1.298(12), N(1)-C(3) 1.244(12), N(3)-C(5) 1.321(12); Cu(1D)-

S(1D) 2.325(2), S(1D)-C(5D) 1.709(10), N(2D)-N(1D) 1.390(11), N(2D)-C(5D)

1.298(12), N(3D)-C(5D) 1.321(12); Cu(1E)-S(1E) 2.325(2), S(1E)-C(5E) 1.709(10),

N(2E)-N(1E) 1.390(11), N(2E)-C(5E) 1.298(12), N(3E)-C(5E) 1.321(12),. Symmetry

Code: D:-0.5+y, 1.5-z, 1-x; E: 1-z, 0.5+x, 1.5-y; E: 1-z, 0.5+x, 1.5-y.

3. Characterizations of Catalysts
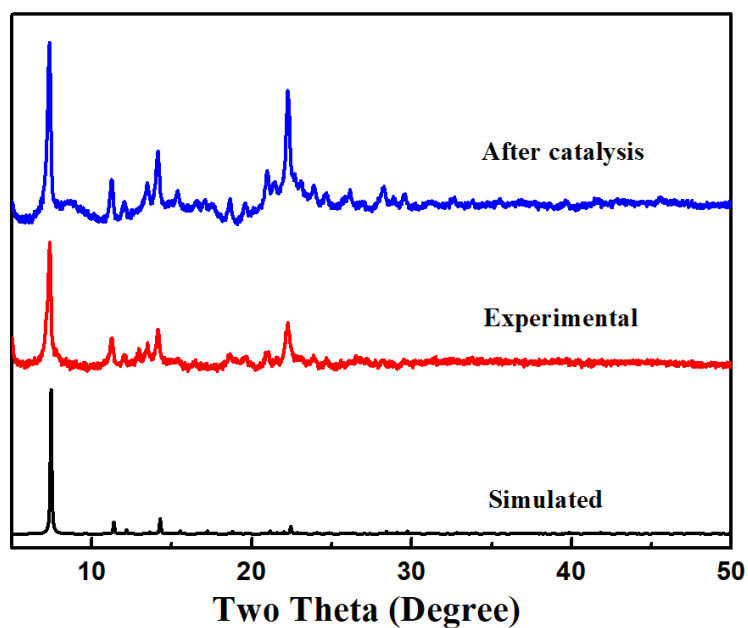
Figure S4. (a) The PXRD spectra. (black bar) Simulated Cu-**TSP**; (red bar) freshly prepared Cu-**TSP**; (blue bar) Cu-**TSP** of after catalysis.
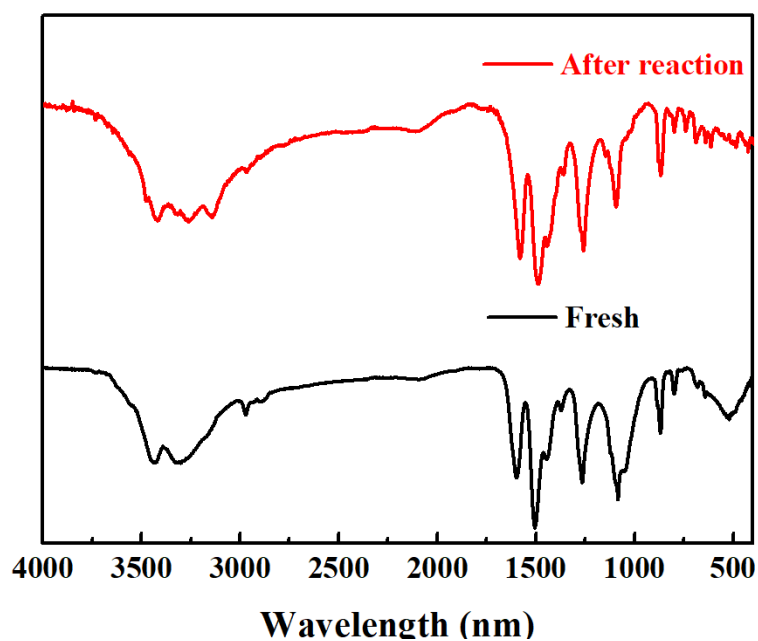

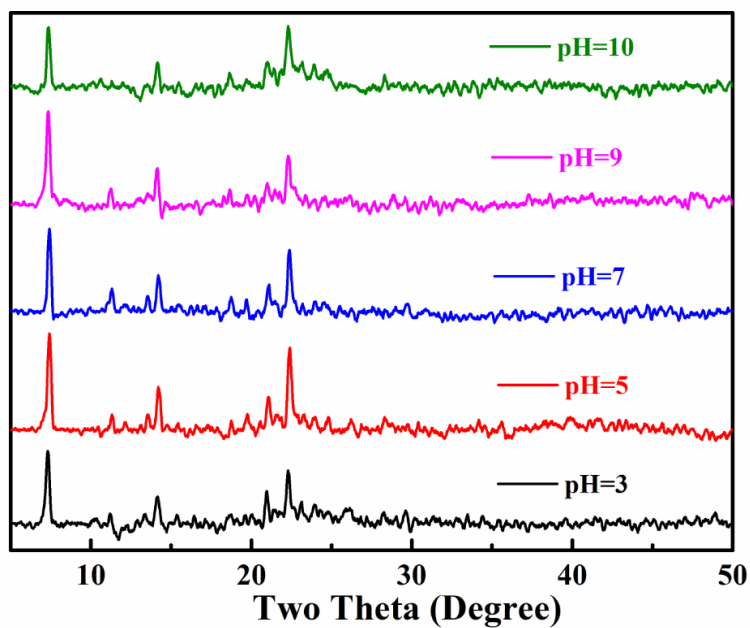**Figure S5**. IR spectra of freshly prepared Cu-**TSP** (black) and Cu-**TSP** after reaction (red).

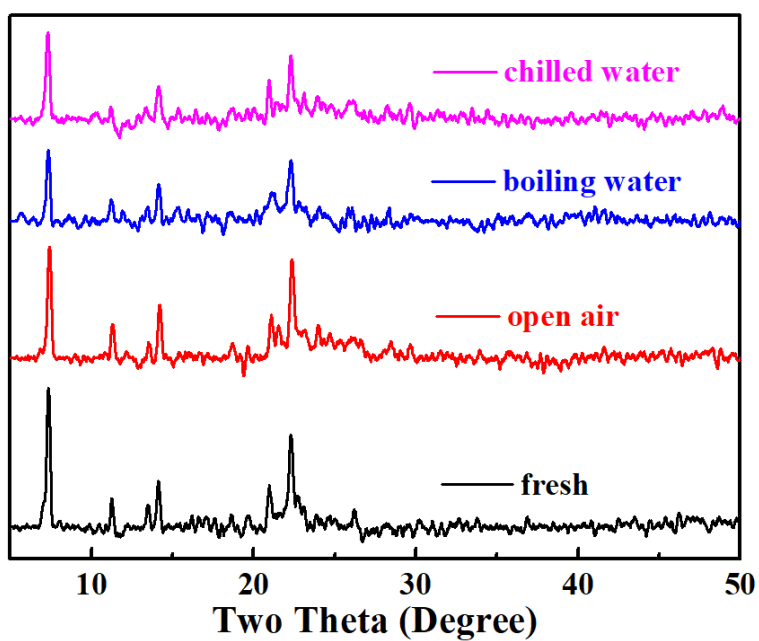**Figure S6.** The PXRD spectra under different pH conditions.

Figure S7. The PXRD spectra. (black bar) fresh; (red bar) open air for prolonged time;

(blue bar) boiling water；   (pink bar) chilled water.
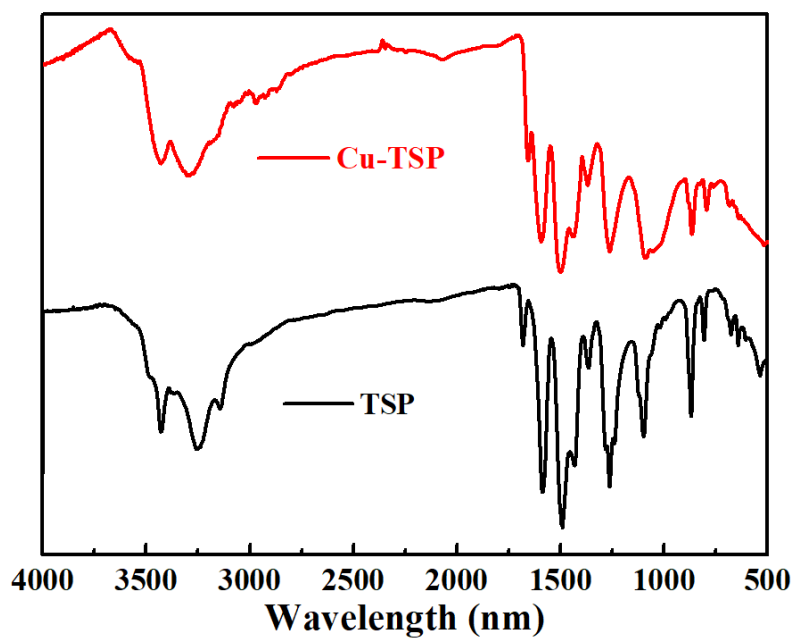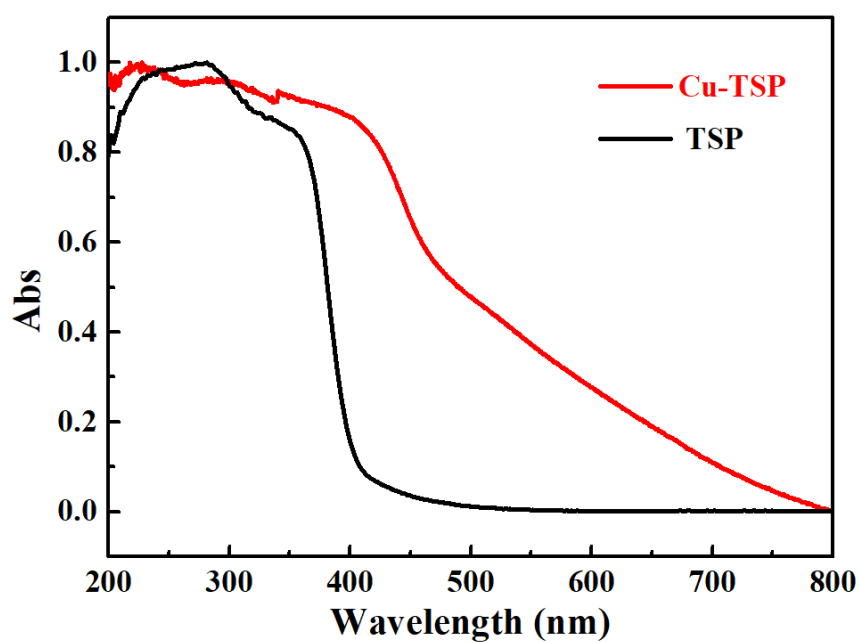
Figure S8. IR spectra of Cu-**TSP** and ligand **TSP**.

Figure S9. UV-*vis* absorption for ground Cu-**TSP** (red line) and **TSP** powder (black line).
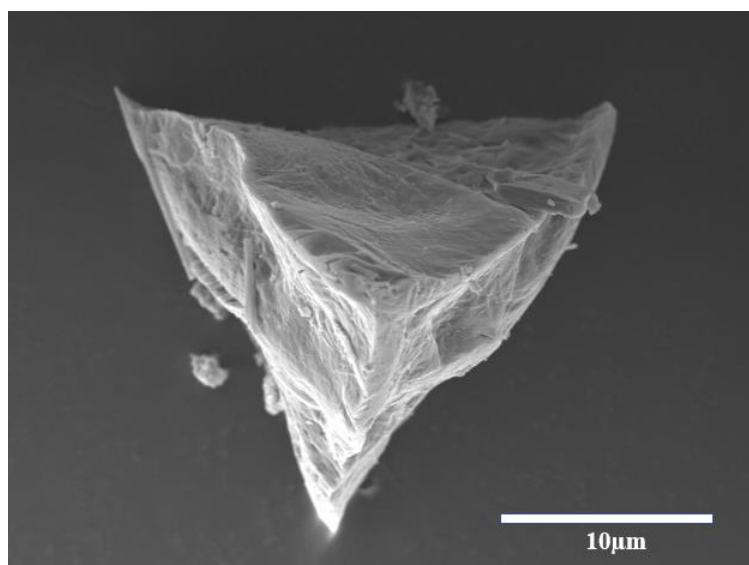
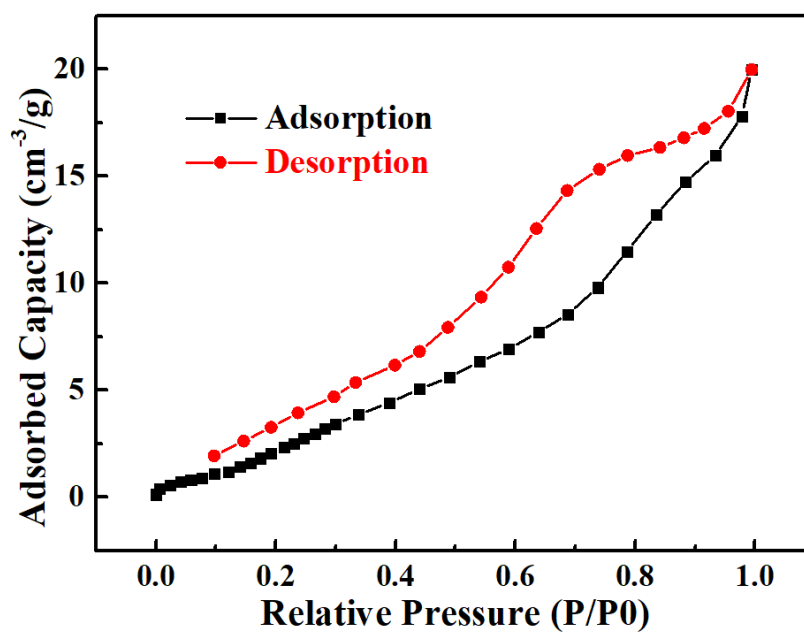**Figure S10**. A magnified SEM image of the as-synthesized photocatalyst Cu-**TSP**.

Figure S11. Nitrogen sorption isotherms for Cu-**TSP** at 77 K.
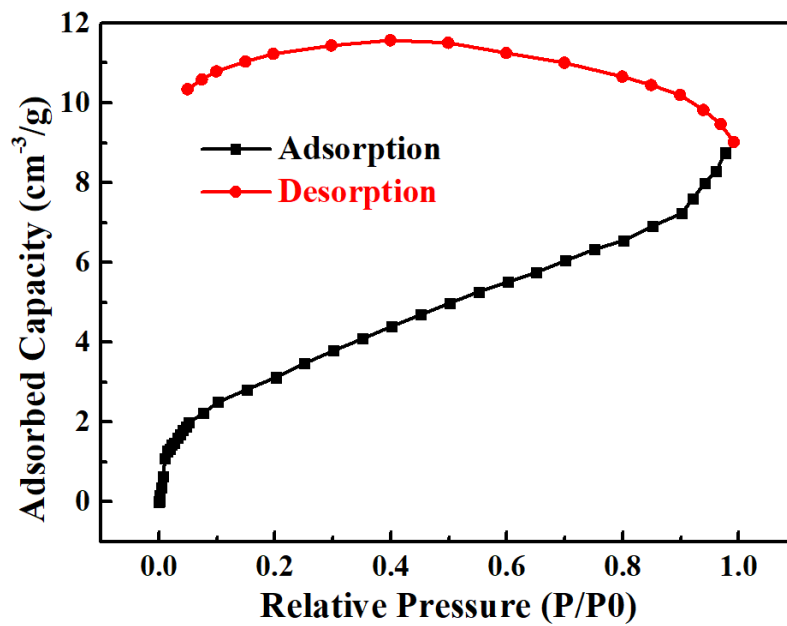
Figure S12. . Carbon dioxide sorption isotherms for Cu-**TSP** at 195 K.
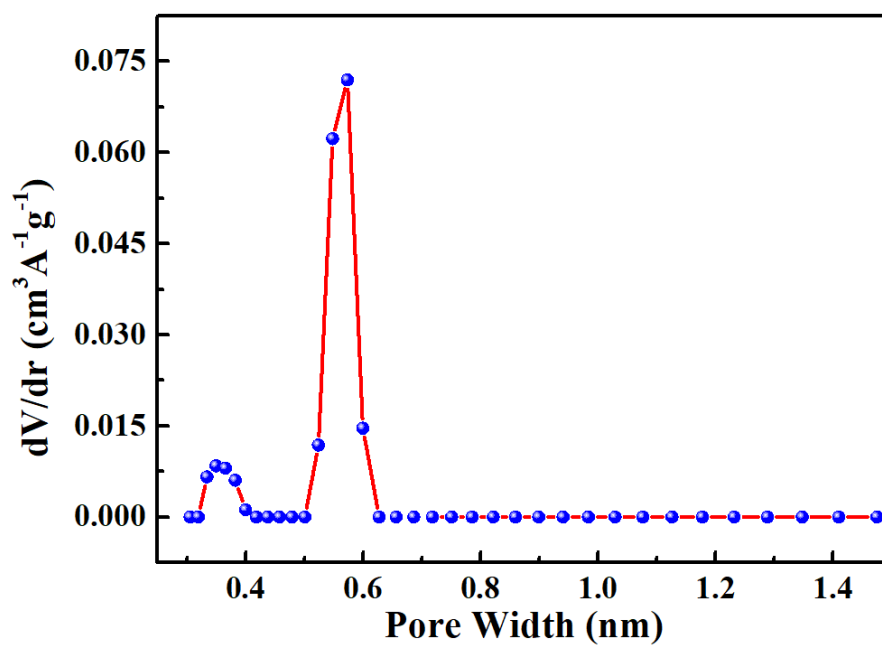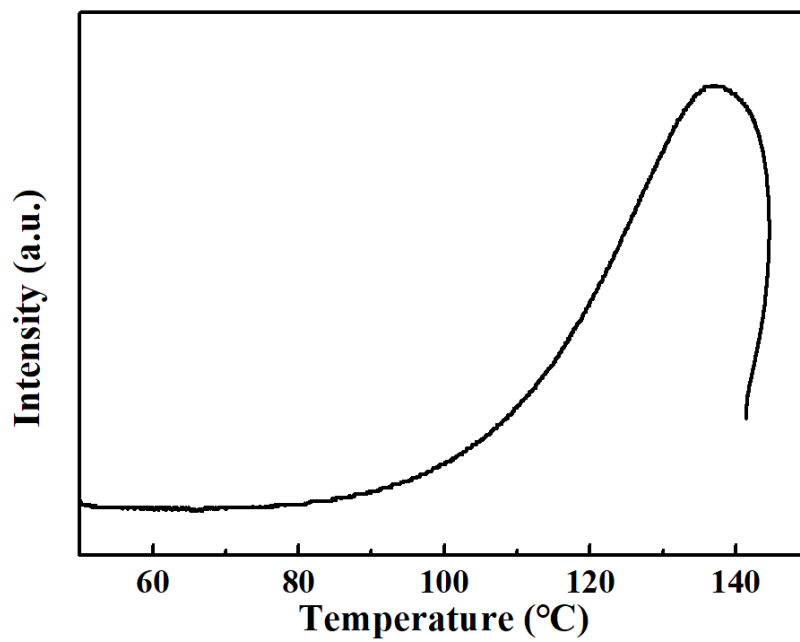

Figure S13. DFT pore size distribution for Cu-**TSP** using data measured with carbon dioxide at 195 K.

```
Total Volume Adsorbed:      347.34 µL
Total Volume @ STP(0C)      312.97 µL
Specific Volume Adsorbed   4822.28 µL/g
Monolayer Uptake:          215.139 µmol/g
```

Figure S14. The CO_2-TPD results of Cu-**TSP.**

Table S2. The results of dye uptake

	Cu-**TSP**
A Crystals+Dye (mg)	15
B Dye concentration (mg/mL)	0.288
The Ratio of Dye Uptake (w/w) (Ratio=B×6ml/(A–B×6ml))	13%

Dye Uptake Method: Before the dye uptake experiments, catalysts were firstly washed with ethyl ester ten times for guest molecular exchange. Then, the wet MOFs crystals were soaked in a methanol solution of malachite green (24mM. 2mL) on an oscillator overnight at room temperature. The resulting crystals were washed with methanol thoroughly to remove the dye from the crystal's surfaces until the solution become colorless, and then dried under a stream of air. The dried-out samples were weighed (A mg). The dried samples were dissociated by concentrated hydrochloric acid (50uL), and the solution was diluted to 6ml with DMF. The absorption experiment was performed on a UV-*vis* spectrophotometer. The concentration of malachite green (B g/L) dye was determined by comparing the UV-*vis* absorption with a standard curve.

Table S3. ICP-OES analysis of the reaction filtrate

Analyte	Concentration	Units	Intensity
Cu 327.393	0.2492	mg/L	230852.9

Table S4. Control experiments for the catalytic carboxylation of propargylic amines with CO_2
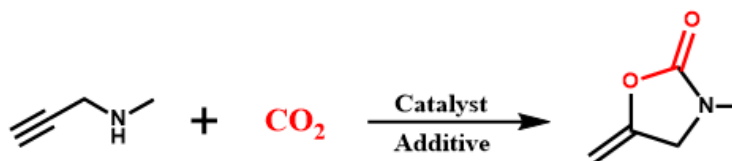
entry	catalyst	base	Temperature (°C)	Yield (%)
1	L	DBU	50	<1
2	none	DBU	50	0
3	L+Cu(CH$_3$CN)$_4$BF$_4$	DBU	50	47
4	Cu(CH$_3$CN)$_4$BF$_4$	DBU	50	46
5	Cu-**TSP**	DBU	50	99
6	Cu-**TSP**	none	50	3
7[b]	Cu-**TSP**	DBU	50	0
8	Cu-**TSP**	DBU	25	61

Reaction conditions: 1a (0.3 mmol), 1 mol % of catalyst (based on Cu), 0.03 mmol (10 mol %) of DBU, CH$_3$CN (3 mL), 50 °C, 24 h, CO_2 (balloon). [b]N$_2$ atmosphere. The yields were determined using ^{1}H NMR spectroscopy.

4. The Summary of MOFs Used in Cycloaddition of Propargylamines

| Catalysts	Amount of Catalyst	Solvent	Temperature	CO_2 Pressure	Time	Yield	Ref.
TNS-Ag8	0.1mmol%	MeCN	25℃	0.1MPa	24h	95%	4
TOS-Ag4	0.1mmol%	MeCN	25℃	0.1MPa	24h	92%	4
Zn_{116}	0.27mol%	MeCN	70℃	0.1MPa	12h	99%	5
NiBDP-AgS	0.5mmol%	DMSO	25℃	0.1MPa	4h	99%	6
TMOF-3-Ag	10mmol%	DMSO	50℃	0.1MPa	12h	97%	7
MOF-1a-Cd	0.01mmol%	MeCN	60℃	0.5MPa	24h	82%	8
Ag-MOF-1	4mmol%	MeCN	25℃	0.1MPa	24h	95%	9
Ag27-MOF	1mmol%	MeCN	25℃	0.1MPa	6h	97%	10
MOF-SO$_3$Ag	0.15mmol%	DMF	25℃	0.1MPa	24h	99%	11
MOF-Cu-Mg	1.4mmol%	MeCN	25℃	0.1MPa	6h	93%	12
Cu$_2$O@ZIF-8	5mmol%	MeCN	40℃	0.1MPa	6h	98%	13
Cu-**TSP**	2mmol%	MeCN	50℃	0.1MPa	24h	99%	This work

5. Catalysis Details

N-methylpropargylamine (1a): The substrate 1a was purchased from Energy Chemical and used without further purification.

N-(prop-2-yn-1-yl)butan-1-amine (2a): The substrate 2a was prepared according to previous reference (Organic Letters, 2016, 18, 5928).
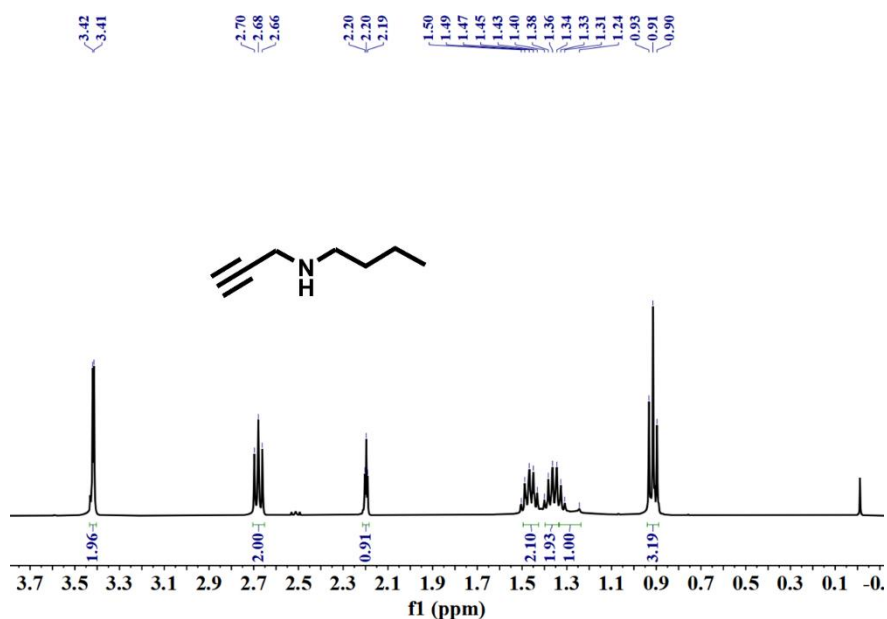
N-(cyclohexylmethyl)prop-2-yn-1-amine (3a): The substrate 3a was prepared according to previous reference (Organic Letters, 2016, 18, 5928).

Synthesis and Characterization of Propargylic Amines (4a-7a): One drop of acetic acid was added to the mixture of propargylamine (12mmol, 0.661g) and benzaldehyde (13mmol, 1.38g) in 20ml methanol. The solution was stirred at room temperature for 24 hours. Then, the mixture was cooled to 0°C, and NaBH$_4$ (18mmol, 0.68g) was added in portions. The mixture was allowed warmed to room temperature and stirred for 1h. The solution was evaporated to dryness and 100mL water was added. The aqueous phase was extracted with CH$_2$Cl$_2$ (50mL×2) and then the organic phase was extracted with 1M HCl (50mL×3). NaHCO$_3$ was added to neutralize the solution and the mixture was extracted with CH$_2$Cl$_2$ (50mL×2). The organic extracts were washed with brine (50mL) and dried (MgSO$_4$). The filtrate was concentrated under reduced pressure, and further purification via silica gel chromatography to afford the pure products.

N-Methylmaleimide (1a): ^{1}H NMR (400 MHz, DMSO-d6) δ 3.23 (d, J = 2.5 Hz, 2H),

3.02 (t, J = 2.4 Hz, 1H), 2.26 (s, 3H), 1.83 (s, 1H).
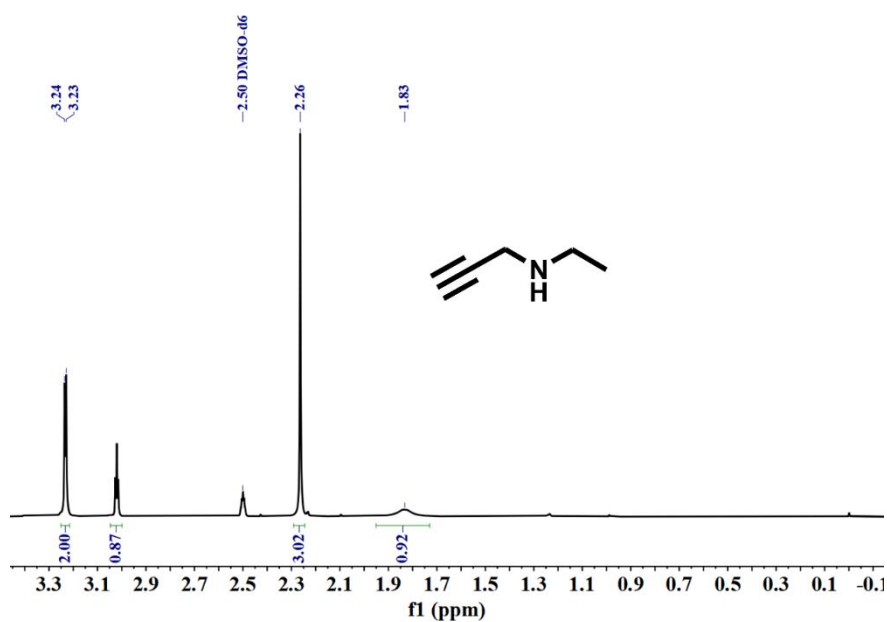
N-(prop-2-yn-1-yl)butan-1-amine (2a): ^{1}H NMR (400 MHz, Chloroform-d) δ 3.42 (d,

J = 2.5 Hz, 2H), 2.68 (t, J = 7.1 Hz, 2H), 2.20 (t, J = 2.4 Hz, 1H), 1.46 (q, J = 7.6, 7.1

Hz, 2H), 1.40 – 1.34 (m, 2H), 1.33 – 1.24 (m, 1H), 0.91 (t, J = 7.3 Hz, 3H).

**N-(cyclohexylmethyl)prop-2-yn-1-amine (3a):** ^{1}H NMR (400 MHz, Chloroform-*d*) δ 3.43 (d, *J* = 2.4 Hz, 2H), 2.63 (tt, *J* = 10.4, 3.8 Hz, 1H), 2.17 (t, *J* = 2.4 Hz, 1H), 1.83 (dd, *J* = 12.3, 3.6 Hz, 2H), 1.71 (dt, *J* = 12.6, 3.6 Hz, 2H), 1.64 – 1.56 (m, 1H), 1.32 – 1.23 (m, 2H), 1.22 – 1.12 (m, 2H), 1.09 – 1.01 (m, 2H).
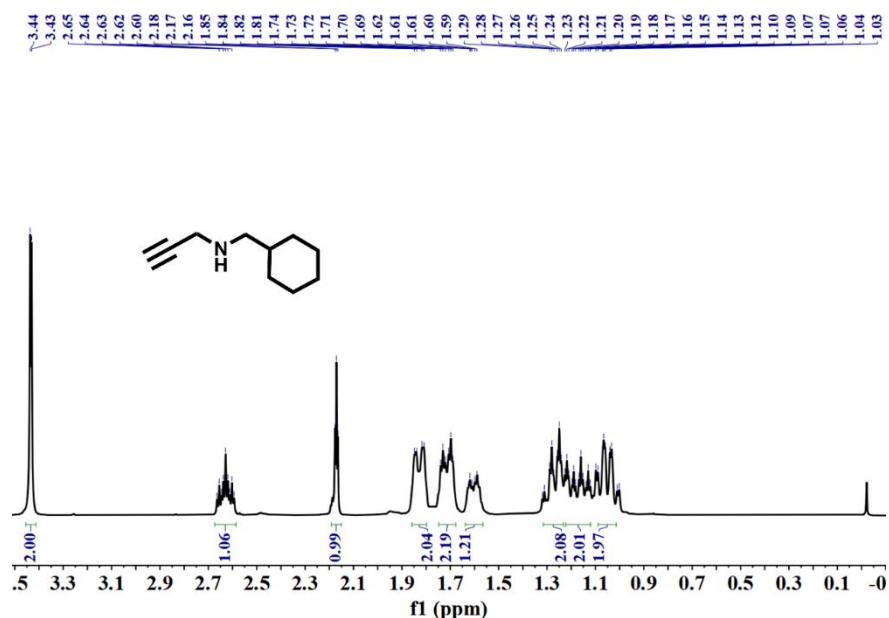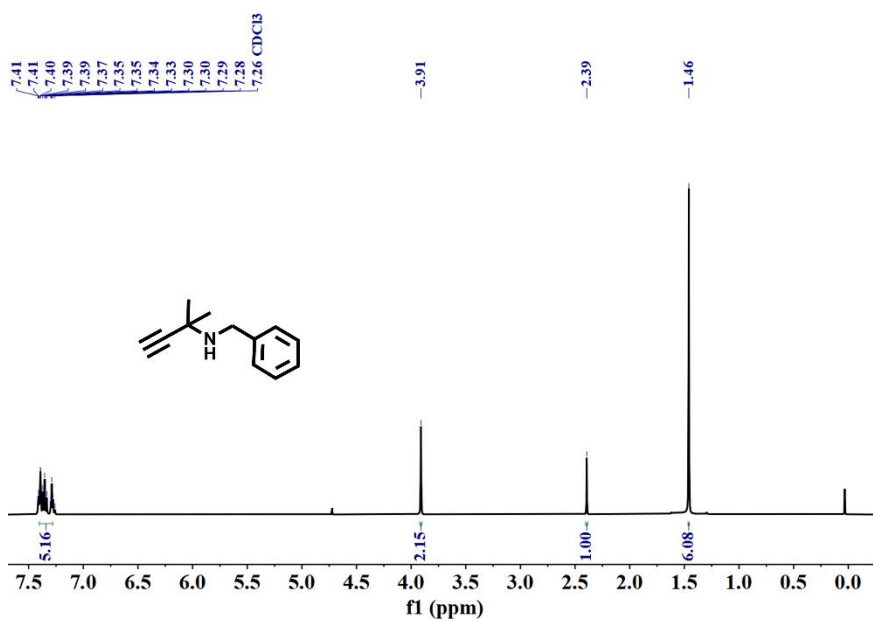

N-(4-nitrobenzyl)prop-2-yn-1-amine (4a): ^{1}H NMR (400 MHz, Chloroform-*d*) δ 8.19 (d, *J* = 8.8 Hz, 2H), 7.54 (d, *J* = 8.7 Hz, 2H), 4.00 (s, 2H), 3.44 (d, *J* = 2.5 Hz, 2H), 2.28 (t, *J* = 2.4 Hz, 1H), 1.59 (s, 1H).
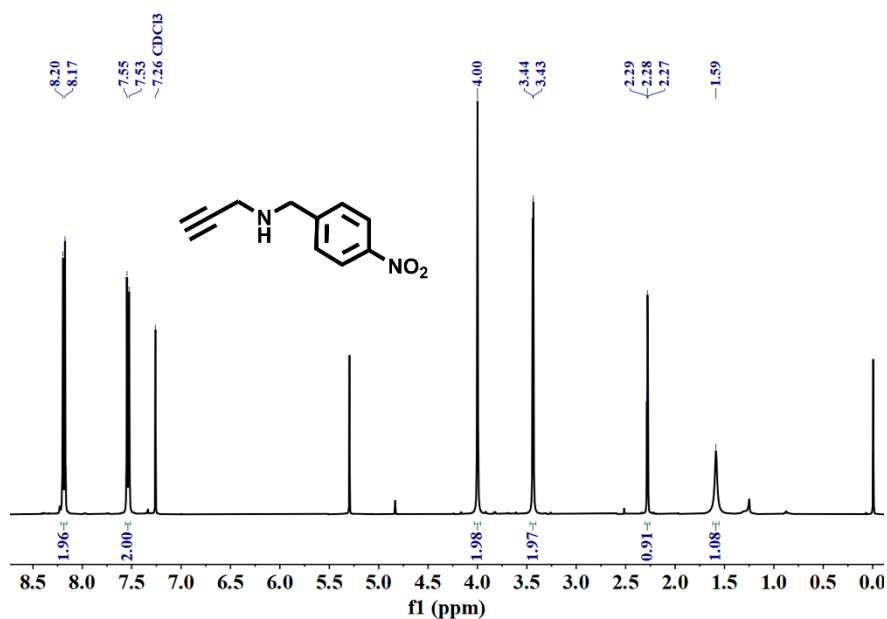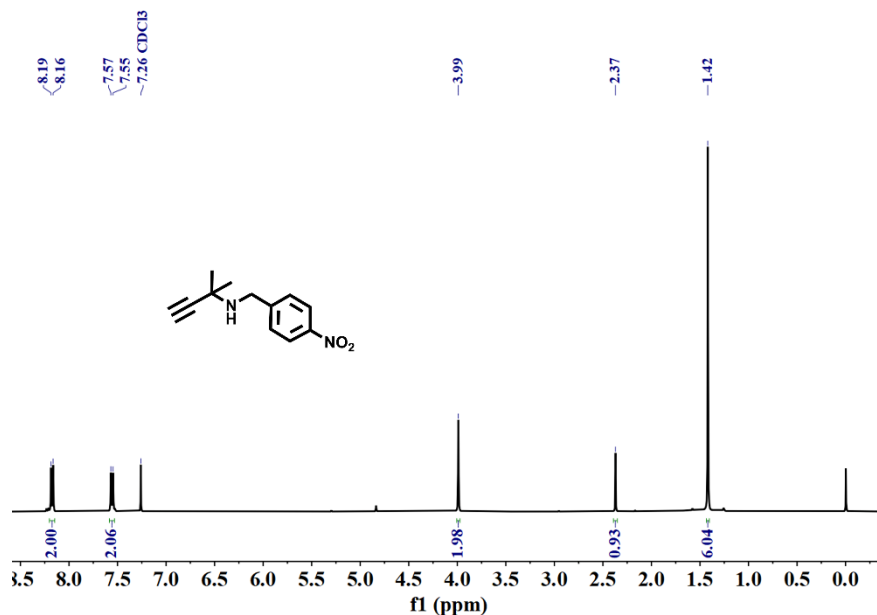
N,N-dimethyl-4-((prop-2-yn-1-ylamino)methyl)aniline (5a): ^{1}H NMR (400 MHz, Chloroform-*d*) δ 7.21 (d, *J* = 8.5 Hz, 2H), 6.72 (d, *J* = 8.5 Hz, 2H), 3.79 (s, 2H), 3.41 (d, *J* = 2.5 Hz, 2H), 2.94 (s, 6H), 2.25 (t, *J* = 2.4 Hz, 1H), 1.78 (s, 1H).
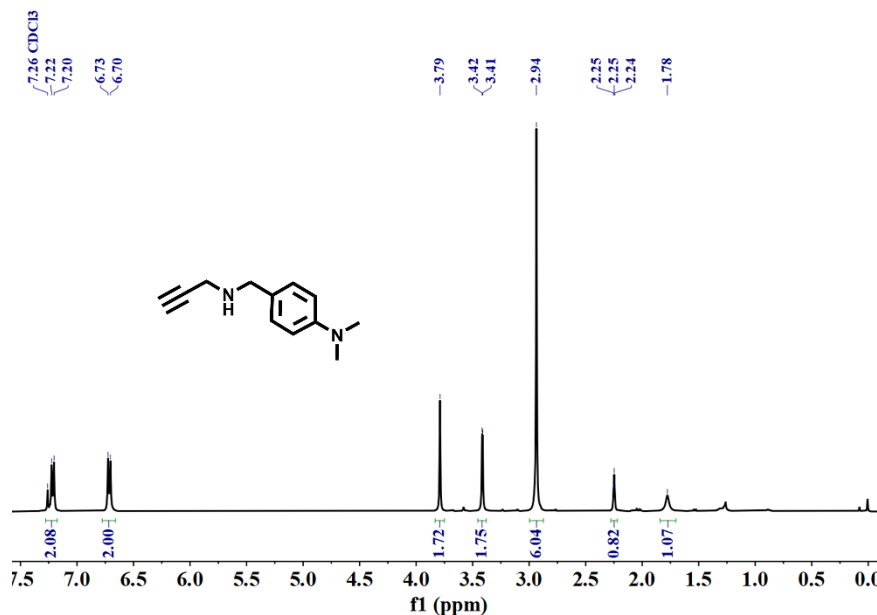

N-benzyl-2-methylbut-3-yn-2-amine (6a): ^{1}H NMR (400 MHz, Chloroform-*d*) δ 7.40 – 7.28 (m, 5H), 3.91 (s, 2H), 2.39 (s, 1H), 1.46 (s, 6H).

2-methyl-N-(4-nitrobenzyl)but-3-yn-2-amine (7a): ^{1}H NMR (400 MHz, Chloroform-*d*) δ 8.20 (d, *J* = 8.7 Hz, 2H), 7.58 (d, *J* = 8.5 Hz, 2H), 4.01 (s, 2H), 2.39 (s, 1H), 1.44 (s, 6H).


4-methyl-N-(4-((prop-2-yn-1-ylamino)methyl)phenyl)-N-(p-tolyl)aniline (8a): ^{1}H NMR (400 MHz, Chloroform-d) δ 7.19 (d, J = 5.2 Hz, 2H), 7.07 – 7.02 (m, 4H), 6.98 (d, J = 3.3 Hz, 6H), 3.83 (s, 2H), 3.46 (d, J = 3.2 Hz, 2H), 2.31 (d, J = 3.4 Hz, 6H), 2.05 (d, J = 3.4 Hz, 1H), 1.27 (s, 1H).
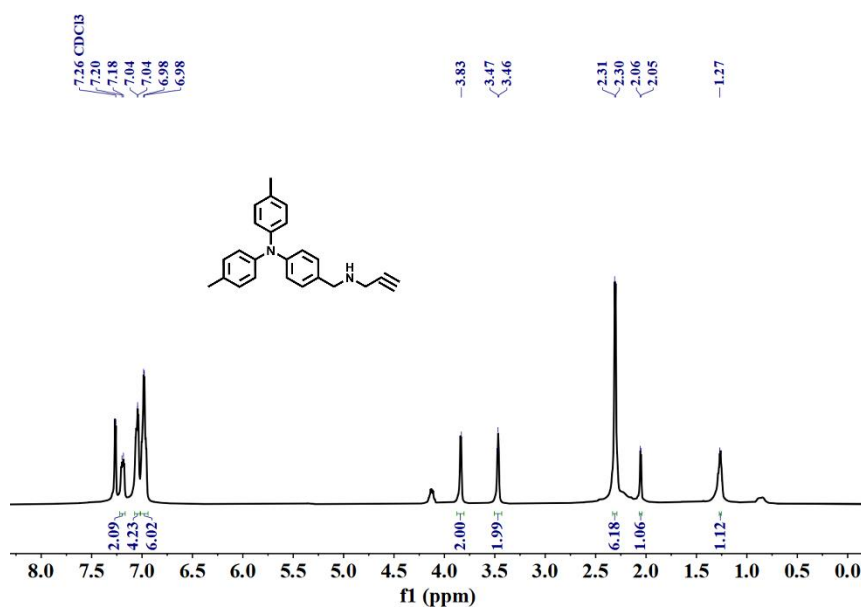
Propargylic Amines Cyclization: Propargylamine (0.3 mmol) and acetonitrile (3 mL), in the presence of 0.03 mmol of DBU and 3.7 mg Cu-**TSP** catalyst, were added in a 10 mL Schlenk tube. The reaction solution was degassed with CO_2 for 10 min, and then, the reaction was sustained with 0.1 MPa CO_2 at 50°C for 1 day. The yields were determined by using ^1H NMR spectroscopy.
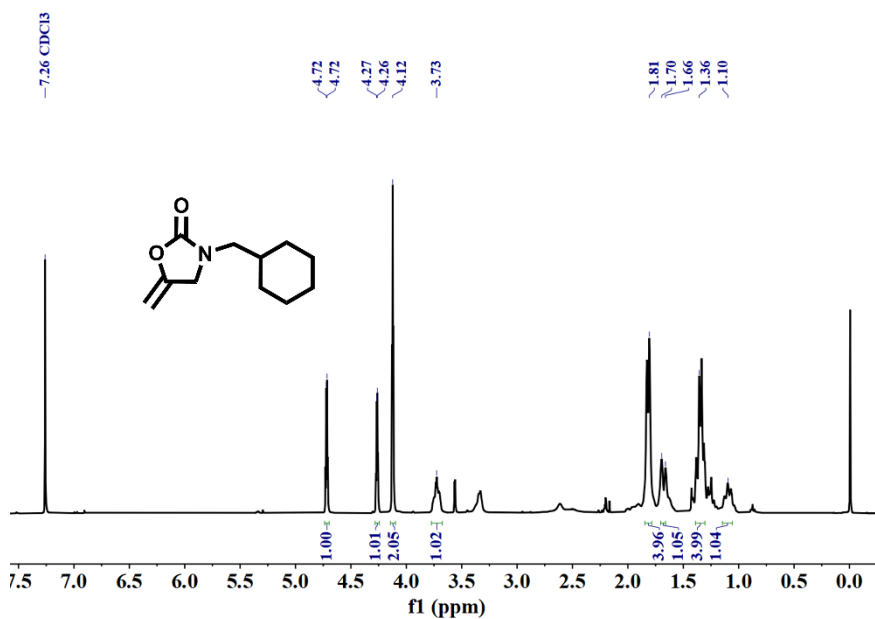
3-methyl-5-methyleneoxazolidin-2-one (1b): ^1H NMR (400 MHz, Chloroform-d) δ 4.74 (q, J = 2.7 Hz, 1H), 4.30 – 4.26 (m, 1H), 4.16 (t, J = 2.4 Hz, 2H), 2.93 (s, 3H).
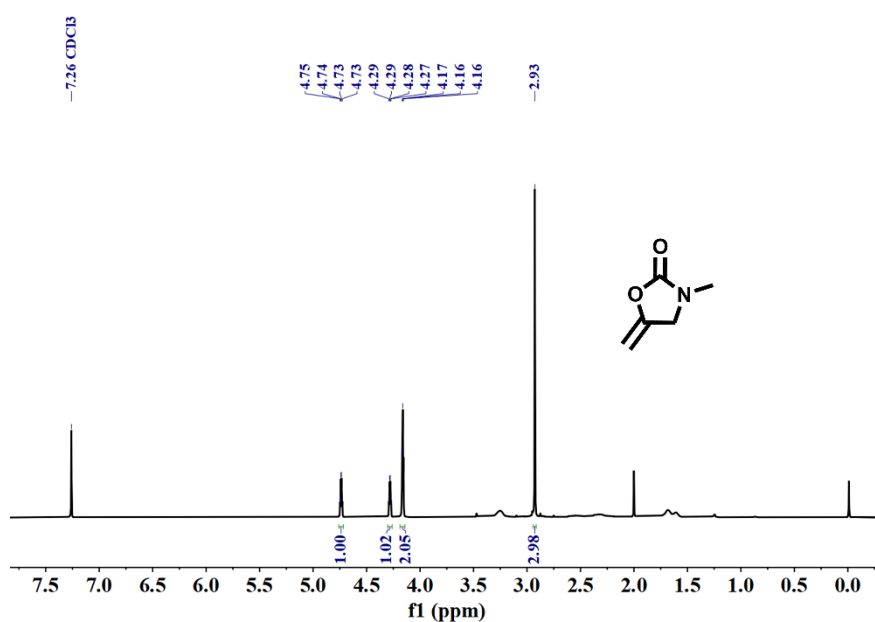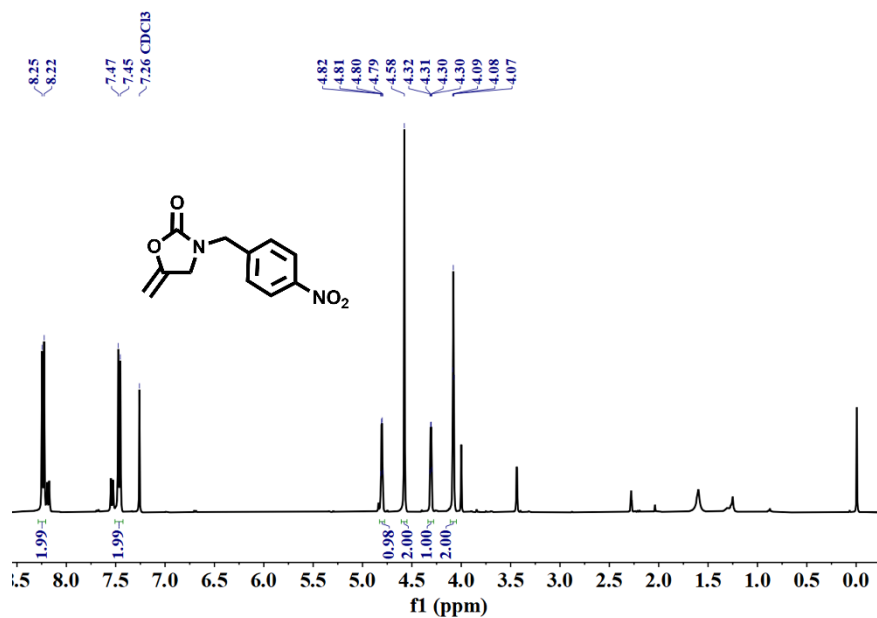
3-butyl-5-methyleneoxazolidin-2-one (2b): ^{1}H NMR (400 MHz, Chloroform-*d*) δ 4.73 (q, *J* = 2.7 Hz, 1H), 4.27 (q, *J* = 2.3 Hz, 1H), 4.15 (t, *J* = 2.4 Hz, 2H), 3.30 (t, *J* = 7.3 Hz, 3H), 1.57 – 1.50 (m, 2H), 1.38 – 1.31 (m, 2H), 0.94 (t, *J* = 7.4 Hz, 3H).
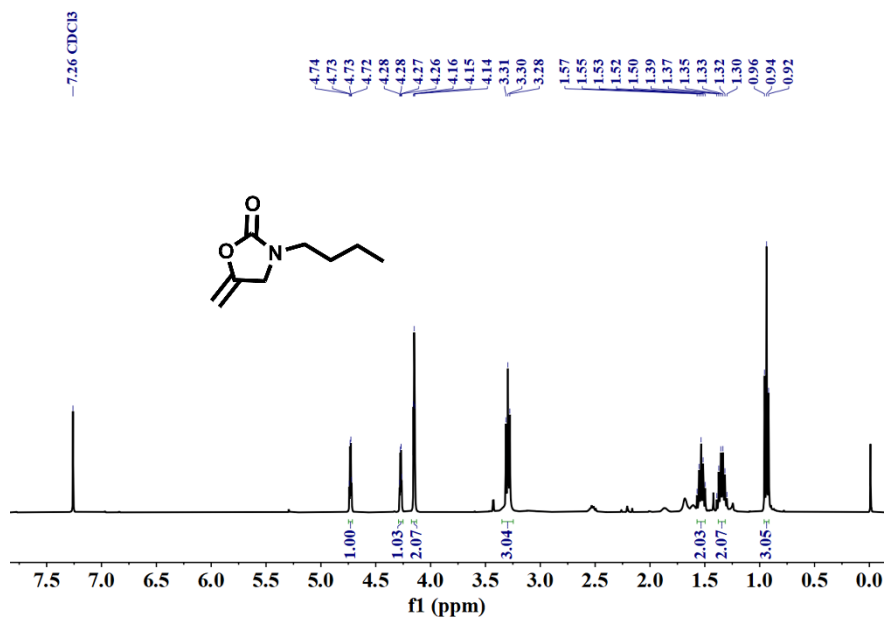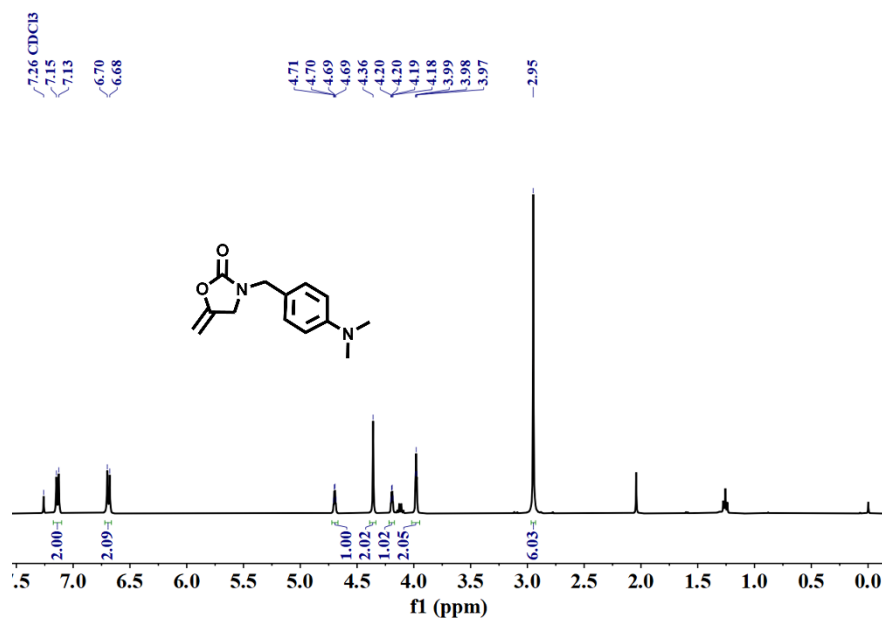

3-(cyclohexylmethyl)-5-methyleneoxazolidin-2-one (3b): ^{1}H NMR (400 MHz, Chloroform-*d*) δ 4.72 (d, *J* = 2.9 Hz, 1H), 4.26 (d, *J* = 2.7 Hz, 1H), 4.12 (s, 2H), 3.73 (s, 1H), 1.84 (s, 4H), 1.68 (d, *J* = 13.8 Hz, 1H), 1.36 (s, 4H), 1.10 (s, 1H).
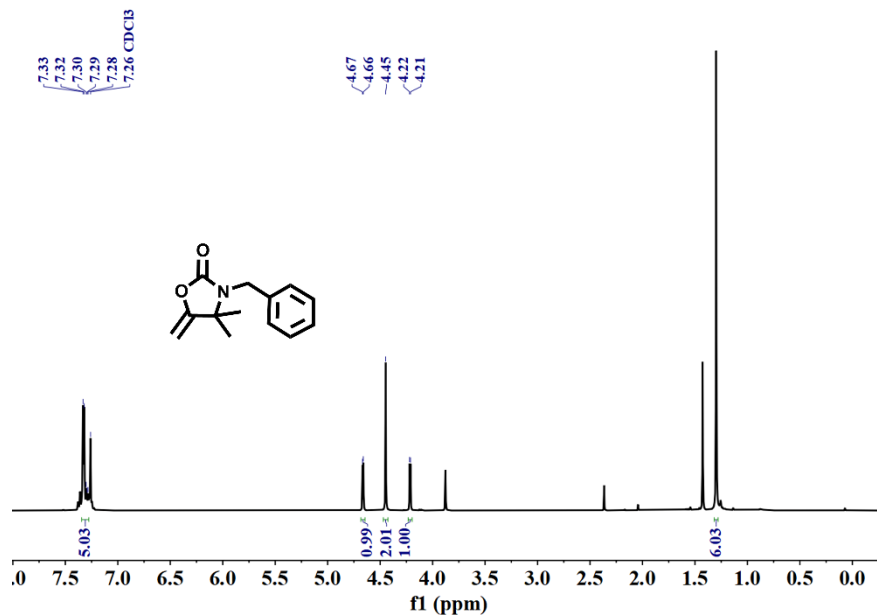
5-methylene-3-(4-nitrobenzyl)oxazolidin-2-one (4b): ^{1}H NMR (400 MHz, Chloroform-d) δ 8.24 (d, J = 8.6 Hz, 2H), 7.46 (d, J = 8.4 Hz, 2H), 4.80 (q, J = 2.9 Hz, 1H), 4.58 (s, 2H), 4.31 (q, J = 2.6 Hz, 1H), 4.08 (t, J = 2.5 Hz, 2H).


3-(4-(dimethylamino)benzyl)-5-methyleneoxazolidin-2-one (5b): ^{1}H NMR (400 MHz, Chloroform-d) δ 7.14 (d, J = 8.6 Hz, 2H), 6.69 (d, J = 8.7 Hz, 2H), 4.70 (q, J = 2.8 Hz, 1H), 4.36 (s, 2H), 4.19 (q, J = 2.4 Hz, 1H), 3.98 (t, J = 2.4 Hz, 2H), 2.95 (s, 6H).

3-benzyl-4,4-dimethyl-5-methyleneoxazolidin-2-one (6b): ^{1}H NMR (400 MHz, Chloroform-*d*) δ 7.33 (d, *J* = 5.0 Hz, 5H), 4.66 (d, *J* = 3.4 Hz, 1H), 4.45 (s, 2H), 4.22 (d, *J* = 3.4 Hz, 1H), 1.30 (s, 6H).

4,4-dimethyl-5-methylene-3-(4-nitrobenzyl)oxazolidin-2-one (7b): ^{1}H NMR (400 MHz, Chloroform-*d*) δ 8.18 (d, *J* = 8.7 Hz, 2H), 7.50 (d, *J* = 8.5 Hz, 2H), 4.71 (d, *J* = 3.5 Hz, 1H), 4.51 (s, 2H), 4.27 (d, *J* = 3.5 Hz, 1H), 1.33 (s, 6H).
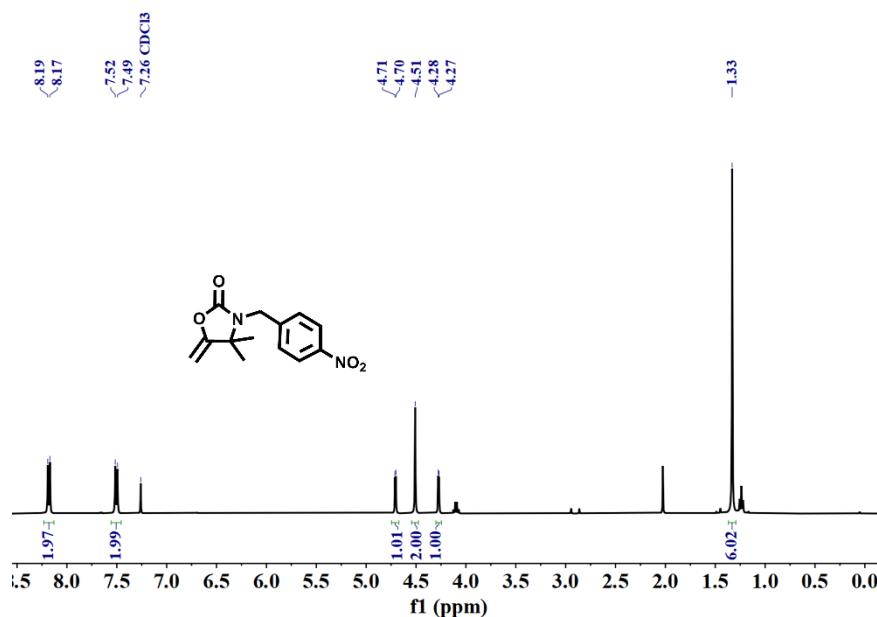
References

1. Luisier, N.; Bally, K.; Scopelliti, R.; Fadaei, F. T.; Schenk, K.; Pattison, P.; Solari, E.; Severin, K. Crystal Engineering of Polymeric Structures with Dative Boron–Nitrogen Bonds: Design Criteria and Limitations. Cryst. Growth Des. 2016, 16, 6600−6604.

2. Sheldrick, G. M. Crystal structure refinement with SHELXL, Acta Crystallogr. Sect. C: Struct. Chem. 2015, 71, 3−8.

3. Spek, A. L. Single-crystal structure validation with the program PLATON, J. Appl. Crystallogr. 2003, 36, 7−13.

4. Z. Chang, X. Jing, C. He, X. Liu and C. Duan, Silver clusters as robust nodes and pi-activation sites for the construction of heterogeneous catalysts for the cycloaddition of propargylamines, ACS Catal., 2018, 8, 1384−1391.

5. C.S. Cao, S.M. Xia, Z.J. Song, H. Xu, Y. Shi, L.N. He, P. Cheng and B. Zhao, Highly efficient conversion of propargylic amines and CO_2 catalyzed by noble-metal-free Zn-116 nanocages, Angew. Chem., Int. Ed., 2020, 59, 8586-8593.

6. H. Yang, X. Zhang, G. Zhang and H. Fei, An alkaline-resistant Ag(I)-anchored pyrazolate-based metal-organic framework for chemical fixation of CO_2, ChemComm, 2018, 54, 4469-4472.

7. G. Y. Zhang, H. M. Yang and H. H. Fei, Unusual missing linkers in an organosulfonate-based primitive-cubic (pcu)-type metal-organic framework for CO_2 capture and conversion under ambient conditions, ACS Catal, 2018, 8, 2519-2525.

8. D. Zhao, X. H. Liu, C. D. Zhu, Y. S. Kang, P. Wang, Z. Z. Shi, Y. Lu and W. Y. Sun, Efficient and reusable metal-organic framework catalysts for carboxylative cyclization of propargylamines with carbon dioxide, Chemcatchem, 2017, 9, 4598-4606.

9 X. Wang, Z. Chang, X. Jing, C. He and C. Duan, Double-helical Ag-S rod-based porous coordination polymers with double activation: δ-active and π-active functions, ACS Omega, 2019, 4, 10828-10833.

10. M. Zhao, S. Huang, Q. Fu, W. Li, R. Guo, Q. Yao, F. Wang, P. Cui, C. H. Tung and D. Sun, Ambient chemical fixation of CO_2 using a robust Ag_{27} cluster-based two-dimensional metal-organic framework, Angew. Chem., Int. Ed., 2020, 59, 20031−20036.

11. R. Das and C. M. Nagaraja, Highly efficient fixation of carbon dioxide at rt and atmospheric pressure conditions: Influence of polar functionality on selective capture and conversion of CO_2, Inorg. Chem., 2020, 59, 9765−9773.

12. A. L. Gu, W. T. Wang, X. Y. Cheng, T. D. Hu and Z. L. Wu, Non-noble-metal metal-organic-framework-catalyzed carboxylative cyclization of propargylic amines with atmospheric carbon dioxide under ambient conditions, Inorg. Chem., 2021, 60, 13425−13433.

13. A. L. Gu, Y. X. Zhang, Z. L. Wu, H. Y. Cui, T.D. Hu and B. Zhao, Highly efficient conversion of propargylic alcohols and propargylic amines with CO_2 activated by noble-metal-free catalyst Cu_2O@ZIF-8, Angew. Chem., Int. Ed., 2022, 61, 14817 −14827.